Journal of Engineering Physics and Thermophysics, Vol. 71, No. 6, 1998

TWO-DIMENSIONAL MODELING OF FILTRATION COMBUSTION IN POROUS CHARGES IN A ONE-TEMPERATURE APPROXIMATION

S. I. Shabunya and V. V. Martynenko

UDC 536.46

Filtration combustion with a stationary front in porous charges is modeled within the framework of a one-temperature approximation. The results of numerical calculations are compared with an analytical evaluation for the quasi-one-dimensional case of a tube of variable cross section.

Introduction. Investigation of combustion in a porous medium using one-dimensional models makes it possible to reveal the basic regularities of this process and to evaluate such important parameters as the maximum temperature and the velocity of the combustion front. However all real technical devices operate under conditions that are rather far from direct application of one-dimensional models. Even in experiments on the propagation of combustion waves in cylindrical tubes with a porous charge [1], regimes with a combustion front tilted to the tube axis often occurred.

Approximate integration of the one-dimensional one-temperature problem of the propagation of a combustion wave with a single-stage Arrhenius-type kinetics of combustion permits derivation of analytical expressions for determining the maximum temperature and the velocity of the combustion wave. Dependences of this type were obtained by different authors, for example, in [2-4]. These expressions are basically distinguished by the method of integrating the Arrhenius exponent. In the present work, we employ the results of the solution proposed in [4], in particular, the formula for determining the area of the combustion front of a steady-state (a zero-velocity wave) solution with a prescribed mass flow rate of the gas. The analytical solutions are based on a one-dimensional approximation, the assumption of homogeneity of the porous medium, and other simplifications. In structures with a variable cross section and inhomogeneous charges and with allowance for the actual thermophysical properties, gas filtration can be substantially non-one-dimensional. In this case, the application of non-one-dimensional numerical models is required. The basic effects of non-one-dimensionality can be analyzed using two-dimensional models. With a two-dimensional description of filtration combustion in a one-temperature approximation we can check and refine the applicability limits for one-dimensional analytical approaches.

Given below is a variant of a two-dimensional one-temperature model that was implemented in the form of a computer code. Using it we compared numerical solutions with the analytical evaluation from [4] and demonstrated some features associated with two-dimensional effects.

Formulation of the Problem and the Method of Solution. The system of equations formulated below describes the following physical processes: gas filtration through a porous medium; convective, conductive, and radiative transfers of heat; energy release in fuel combustion described using the Arrhenius approximation. The gaseous medium is considered in the ideal-gas approximation. As a generalized filtration law, we used the Darcy equation in the form proposed by Forchheimer [5]

$$\nabla P = -\frac{\mu}{k}\mathbf{u} + \frac{\rho_g}{k_1}|\mathbf{u}|\mathbf{u}, \tag{1}$$

Academic Scientific Complex "A. V. Luikov Heat and Mass Transfer Institute of the National Academy of Sciences of Belarus," Minsk, Belarus. Translated from Inzhenerno-Fizicheskii Zhurnal, Vol. 71, No. 6, pp. 963-970, November-December, 1998. Original article submitted February 11, 1998.

1062-0125/98/7106-0925$20.00

$$\rho_g = \frac{PM}{R_g T}, \tag{2}$$

$$\operatorname{div}(\rho_g \mathbf{u}) = 0, \tag{3}$$

$$(1 - \varepsilon_p)\, c_s \rho_s \frac{\partial T}{\partial t} + c_g (\rho_g \mathbf{u} \cdot \nabla T) = \operatorname{div}(\lambda_s \nabla T) + H \rho_g KC \exp\left(-\frac{U}{T}\right), \tag{4}$$

$$\operatorname{div}(\rho_g \mathbf{u} C) = -\rho_g KC \exp\left(-\frac{U}{T}\right), \tag{5}$$

where C is the dimensionless concentration normalized to the quantity of fuel in the initial mixture. The heat of combustion H is calculated as a function of the quantity of fuel in the initial mixture. To describe the radiative heat transfer, we use a diffusion approximation. The effective thermal conductivity λ_s is the sum of the conductive and radiative terms, which depend on the bulk porosity ε_p and the diameter of the charge grains D [6]:

$$\lambda_s = (1 - \varepsilon_p)\lambda_m + \frac{32\sigma D \varepsilon_p}{9(1 - \varepsilon_p)} T^3. \tag{6}$$

For computer implementation, the initial system of equations (1)-(5) was transformed. The combination (1)-(3) yields the elliptical equation

$$\operatorname{div}\left(\frac{k \nabla P^2}{2\left[\frac{\mu R_g T_g}{M} + P\,|\mathbf{u}|\,\frac{k}{k_1}\right]}\right) = 0 \tag{7}$$

to find the pressure distribution. We transformed the energy equation (4) to the form

$$(1 - \varepsilon_p)\, c_s \rho_s \frac{\partial T}{\partial t} = \operatorname{div}(\lambda_s \nabla T - H \rho_g \mathbf{u} C) - c_g (\rho_g \mathbf{u} \cdot \nabla T). \tag{8}$$

And, in Eq. (5), we went over to the variable ln C to avoid numerical difficulties in integrating near zero concentration

$$(\rho_g \mathbf{u} \cdot \nabla \ln C) = -K \exp\left(-\frac{U}{T}\right). \tag{9}$$

The initial temperature distribution was prescribed in such a manner as to ensure ignition of the fuel mixture. We consider two configurations of the computational domain (Fig. 1): the boundary conditions for the computational domain shown in Fig. 1a:

$$\left.\frac{\partial P}{\partial n}\right|_{I} = 0, \quad \left.\lambda_s \frac{\partial T}{\partial n}\right|_{I} = \alpha_I (T - T_0) + \varepsilon_I \sigma (T^4 - T_0^4);$$

$$P|_{II} = p_0, \quad \left.\lambda_s \frac{\partial T}{\partial n}\right|_{II} = 0; \tag{10}$$

$$\left.\frac{\partial P}{\partial n}\right|_{III} = 0, \quad \left.\lambda_s \frac{\partial T}{\partial n}\right|_{III} = \alpha_{III} (T - T_0) + \varepsilon_{III} \sigma (T^4 - T_0^4);$$

$$P|_{IV} = p_{in}, \quad \ln C|_{IV} = 0, \quad T|_{IV} = T_0;$$

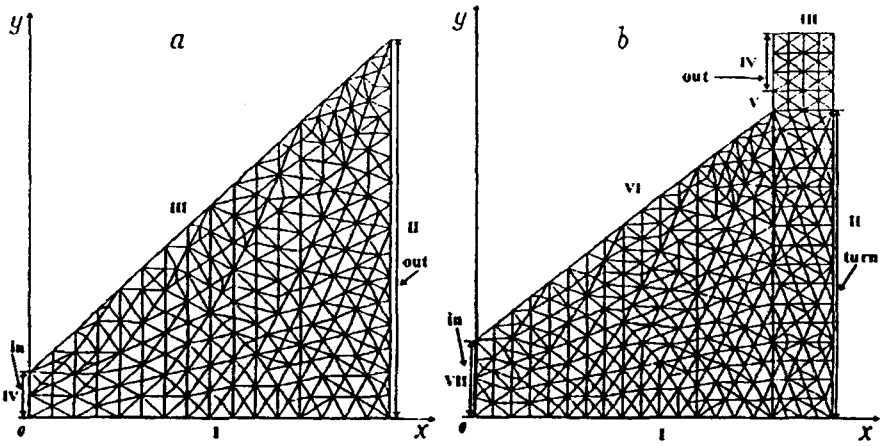

Fig. 1. Schemes of computational domains: filtration in the regime of direct flow (a) and with a turn of the gas flow (b).

the boundary conditions for the computational domain shown in Fig. 1b:

$$\left.\frac{\partial P}{\partial n}\right|_{I} = 0, \quad \lambda_s \left.\frac{\partial T}{\partial n}\right|_{I} = 0;$$

$$\left.\frac{\partial P}{\partial n}\right|_{II} = 0, \quad \lambda_s \left.\frac{\partial T}{\partial n}\right|_{II} = \varepsilon_{II}\sigma(T^4 - T_0^4);$$

$$\left.\frac{\partial P}{\partial n}\right|_{III} = 0, \quad \lambda_s \left.\frac{\partial T}{\partial n}\right|_{III} = 0;$$

$$P_{IV} = p_0, \quad \lambda_s \left.\frac{\partial T}{\partial n}\right|_{IV} = 0; \tag{11}$$

$$\left.\frac{\partial P}{\partial n}\right|_{V} = 0, \quad \lambda_s \left.\frac{\partial T}{\partial n}\right|_{V} = 0;$$

$$\left.\frac{\partial P}{\partial n}\right|_{VI} = 0, \quad \lambda_s \left.\frac{\partial T}{\partial n}\right|_{VI} = 0;$$

$$P|_{VII} = p_{in}, \quad \ln C|_{VII} = 0, \quad T|_{VII} = T_0.$$

To ensure a constant flow rate, we adjusted iterationally the pressure p_{in} at the inlet boundary on each time step and took the pressure at the outlet from the system p_0 to be equal to atmospheric pressure.

A solution of the problem was found numerically in the following order. Equation (7) was solved for the pressure, and the modulus of the velocity and the temperature were taken from the previous time step. To find the logarithm of the concentration, we integrated the hyperbolic equation (9) along the characteristics using the velocity and temperature field obtained from the previous time step. Then we performed the next time step for the energy equation (8). The initial temperature distribution evolves either to a steady-state solution if the parameters of the problem fall within the region of existence of these solutions or the reaction front leaves the computational domain.

Equations (7) and (8) were solved by the finite-element method on a fixed grid. As a rule, from 500 to 1000 triangular elements were used. The division of the domains into the triangles is shown in Fig. 1. Equation (9) was integrated along the characteristics with an adaptive step that provides the required accuracy. In the case of steady-state solutions, the mass-energy balance relations were fulfilled with an error of less than 1%.

Results of Numerical Modeling. The quasi-one-dimensional analysis performed in [4] for the case of a tube of variable cross section enables us to find the position of the stationary combustion zone, for which the combustion-wave velocity becomes zero. In this case, the position of the combustion front, with the prescribed mass flow rate m and the temperature increment due to the combustion ΔT_{ad}, corresponds to the cross-sectional area S_1 expressed in terms of the parameters of the process in the following manner:

$$S_1 = m\left[\frac{\exp\left(U/(T_0+\Delta T_{ad})\right) HU}{\lambda K \rho_0 T_0 (T_0+\Delta T_{ad})}\left(1-\frac{(T_0+\Delta T_{ad})\ln 2}{U\Delta T_{ad}}(2T_0+\Delta T_{ad})\right)\right]^{1/2}. \quad (12)$$

This one-dimensional analysis for a tube of variable cross section cannot allow for the special features of gas filtration and is based only on a constant flow rate in each cross section. In this case, the cross-sectional area S_1 does not depend on the rate of opening of the filtration channel. The shape of the front produced will be plane, which is natural for the one-dimensional theory but disagrees with the actual pattern of filtration combustion.

With the aim of checking the conclusions of the analytical evaluation from (12) we performed a series of calculations under adiabatic conditions for direct-flow systems with different apex angles that varied from 1 to 41°. The calculations were performed for charges with a bulk porosity $\varepsilon_p = 0.5$ and a charge-grain diameter $D = 10^{-3}$ m in combustion of a fuel mixture whose calorific power H was $1.26 \cdot 10^6$ J/kg.

In all cases, when the stationary cross section predicted by the analytical expression (12) was within the computational domain the numerical solution converged to the steady-state solution. Unlike the one-dimensional theory, the shape of the front was not plane in the calculations. In the numerical calculations, a surface of identical concentration that was 1% of the inlet concentration was meant by the front. The surface area was defined as the product of the length of the line that links the points of equal concentration by a length of 1 m in the z direction, perpendicular to the computational domain. Whereas at small apex angles (1–10°) the front was nearly plane, with increase in this angle the bend of the front became increasingly pronounced. However the area of the bent front coincides with the analytical value, which was observed for the entire range of apex angles considered and all mass flow rates that ensure steady-state regimes for the prescribed geometry of the computational domain. Calculations for larger apex angles were not performed since this was not required by the technical device for which the model was developed. In principle, this modeling can be performed but it requires a change in the part of the numerical procedure associated with implementation of the boundary conditions.

Direct application of the constants of the gross kinetics of a gaseous-phase reaction for the present model is not correct for two reasons. First, because of the intense interphase heat transfer the behavior of the temperature of the gaseous phase in the porous body differs strongly from the case of a premixed laminar flame that propagates in a free space, which in turn leads to a change in the channels of the elementary reactions occurring. Second, for a one-temperature approximation there is no abrupt temperature change in the gas in the reaction zone, which also requires overdetermination of the kinetic constants to ensure agreement of the numerical results with the experimental data.

For modeling the combustion reaction, we used the following values of the constants of the gross kinetics: $U = 15{,}640$ K for the activation energy and $K = 4.6 \cdot 10^6$ sec^{-1} for the preexponential factor. The first corresponds to the energy of methane activation that is widely used in similar calculations [7-9], while the magnitude of the second is chosen in the process of working on comparing calculated data with results of experiments performed in our laboratory. The quantity K was determined by an original procedure using a complete kinetic model for the set of parameters characteristic of the experimental conditions. A detailed presentation of the procedure is not the subject of this work and therefore is not given here. Use of these values yielded acceptable agreement of the calculations with the experimental data on the temperatures and the areas of the stationary fronts. However the value selected for K is not universal and is applicable only to a concrete set of parameters of the system.

With the aim of analyzing the effect of heat losses on the shape of the combustion front we performed calculations for conditions that are different from adiabatic conditions. The profiles of the combustion front presented in Fig. 2 demonstrate results of calculation in the case of heat losses on the upper (Fig. 2a) and lower (Fig. 2b) lateral surfaces. For a qualitative comparison, the profiles of the steady-state combustion front under

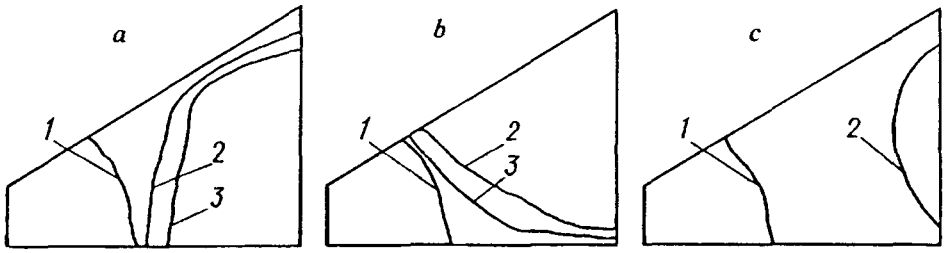

Fig. 2. Effect of heat losses on the shape of the front of steady-state combustion with cooling of the upper [a: 1) adiabatic conditions, 2) α = 50 W/(m^2·K), 3) 90], lower [b: 1-3) the notation is the same as in a)], and both lateral surfaces [c: 1) adiabatic conditions, 2) α = 80 W/(m^2·K)] by convective heat transfer and radiation with an emissivity factor ε = 0.7.

adiabatic conditions are shown on each. It can easily be seen from the figure that cooling of the wall induces growth of the area of the front and its displacement downstream. The calculation of the problem with cooling can be interpreted to a certain degree as a calculation under adiabatic conditions with a lower calorific power of the fuel. However we cannot directly compare the results of the numerical calculation with the analytical evaluation since loss of heat leads to the profile of the front being strongly distorted. From Fig. 2a and b it can be seen that it becomes concave and significantly displaced downstream in the region adjacent to the cooled lateral surface. Figure 2c shows the variant of calculation in the case of heat losses on both lateral surfaces, for which the emissivity factors and the coefficients of heat removal were assumed to be the same and were 0.7 and 80 W/(m^2·K), respectively. Under these conditions of cooling, a steady-state regime with incomplete combustion of the fuel was realized. Approximately 30% of the unburned fuel escaped along the cold walls.

The direct-flow system is characterized by monotonic behavior of the cross section. This makes it possible to stabilize the position of the combustion front in a cross section that depends on the mass flow rate of the gas. The developed computer model was tested on this region. The calculations were performed to compare results with allowance for the two-dimensional character of the filtration and analytical results for the quasi-one-dimensional case [4]. However the computer model was developed for investigating concrete technical applications that require two-dimensional analysis of filtration combustion for different configurations of real devices with nonmonotonic behavior of the flow section. A model with a turn of the gas flow was one variant (see Fig. 1b). The prime objective of such an investigation is analysis of the emitting efficiency of surface II. From the viewpoint of filtration, the system with a turn is much more complicated than the direct-flow system. The geometry of the direct-flow system is characterized by the following quantities: the dimensions of the inlet S_{in} and outlet S_{out} cross sections and the length of the region. Only the cross sections can be considered important geometric parameters for front stabilization. The geometric and regime parameters must be selected so as to satisfy the following condition between S_{in} and S_{out} and the stationary-front cross section determined analytically (12):

$$S_{in} < S_1 < S_{out}. \tag{13}$$

Only in this case is it possible to stabilize the front of the steady-state combustion within the region. If condition (13) is not satisfied the combustion either reaches the inlet surface or decays. Indeed, numerical modeling showed that, for parameters for which $S_1 > S_{out}$, the combustion wave became concurrent and the system decayed. If the parameters were prescribed in such a manner that $S_{in} \approx S_1$, the combustion front was counter-moving. We should note that with combustion on the inlet surface it is not correct to prescribe a constant inlet temperature. However these regimes were not the subject of investigation. Modeling with specification of S_{in} that was similar to S_1 was performed only to demonstrate the predicted evolution of the combustion front.

Estimate (13) is a very useful recommendation in determining structural parameters of technical devices. Beyond that, it will help to find immediately the limiting regimes of combustion with a stationary front for existing direct-flow devices as an upper bound. The use of (12) simultaneously with (13) enables us to contract significantly the range of design parameters, should the need for optimization calculations arise.

TABLE 1. Cross Sections of the Front of Steady-State Combustion Obtained Analytically S_1 and Numerically S_{num} for Different Mass Flow Rates of the Gas Flow

G, kg/sec	S_1, m^2	S_{num} ($C=0.01$), m^2
0.0144	0.061	0.07
0.02	0.084	0.09
0.0256	0.106	0.12
0.0339	0.135	

Calculations on the scheme with a turn revealed regularities associated with the geometry of the flow. We should note that, unlike the direct-flow system, the system with a turn of the gas flow has more characteristic dimensions. If the parameters of the system are such that the cross sections of the outlet orifice S_{out} and the turning portion S_{turn} are larger than the cross-sectional area for a stable regime S_1, this situation, in terms of stability, does not differ from the direct-flow system. However depending on the selection of the turn geometry a situation can occur where the relation of the cross sections in the turn and at the outlet can have a substantial effect on the stability. If one of the two cross sections is smaller than the cross section of the stable regime, the situation requires additional analysis. Use of the analytical evaluation (12) in these cases does not make it possible to predict the behavior of the system. Therefore we need to perform a series of calculations to determine the limits for stable regimes, the more so under nonadiabatic conditions.

Table 1 gives data for four different mass flow rates of the gas for the system with a turn of the gas flow. A series of calculations performed for all these flow rates in the direct-flow system showed that stable regimes are realized in it. The areas of the combustion front that correspond to the data obtained analytically S_1 and calculated numerically S_{num} are indicated in the table.

As the table shows, the first three regimes in the system with a turn of the flow proved stable, while the fourth regime lost stability. It should be noted that, in all four cases, the cross-sectional area in the front is larger than the area predicted by the one-dimensional theory. The reasons for this are apparently due both to the presence of heat losses (radiation from surface II) and the character of the filtration. In the system with a turn of the gas flow, the lower right corner of the design domain is characterized by attenuated filtration. The current tubes first diverge but then converge. By the flow cross section by which the stability should be evaluated, we should mean the surface perpendicular to the current lines with the maximum area. If the cross section required for the existence of a steady-state regime is smaller than the maximum cross section, the regime will be stable. For simple cases, this evaluation can be made from geometric considerations. In the case of inhomogeneous charges, the actual pattern of the current lines depends on numerous parameters of the system and is difficult to predict in advance without performing calculations. In this situation, we have to resort to a numerical calculation to determine the limit of stable regimes.

The results described above are in agreement with numerical calculations performed for both configurations with a uniform permeability of the porous charge. However, in real technical devices, the charges can be inhomogeneous. The effect of inhomogeneity on the filtration pattern can be very substantial. The synthesized algorithm makes it possible to model processes for systems with nonuniform properties.

Given below is a series of calculations for inhomogeneous porous charges. Figure 3a presents a variant of the configuration of the computational domain with zones, denoted by 1 and 2, in which we can prescribe different characteristics of the process, such as permeability, porosity, and thermal conductivity. The number of zones and their configuration can be arbitrary within the framework of the division of the computational domain into finite elements. The effect of the inhomogeneity of the porous charge on the character of the filtration is demonstrated by the following series of calculations. Zone 1 was filled with grains of diameter $D = 10^{-3}$ m while the grain diameter in zone 2 was varied and was, respectively, 10^{-3}, $5.5 \cdot 10^{-4}$, and $2 \cdot 10^{-4}$ m. The calculations were performed for the case of adiabatically isolated surfaces I and IV and radiation from surface II with an emissivity factor of 0.7. With a uniform permeability (Fig. 3b), the flow rate in the system is distributed in such a manner that the lower

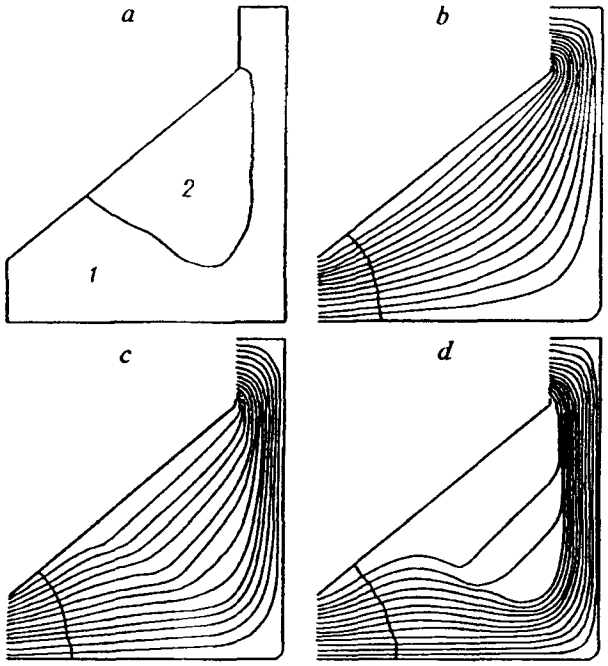

Fig. 3. Division of the computational domain into two zones (a, 1, 2) and profiles of current lines and the combustion front for charges with grain diameters in zone 2 of 10^{-3} m (b), $5.5 \cdot 10^{-4}$ m (c), and $2 \cdot 10^{-4}$ m (d).

right corner is stagnant. The deterioration of the permeability in zone 2 leads to the flow being pressed out of the region with poor permeability. With decreasing permeability in zone 2 the profile of the current lines becomes more and more bent (Fig. 3c) and it can occur that, actually, the entire flow is filtered only through zone 1 (Fig. 3d). In the case where the steady-state cross section occurs in zones with dissimilar permeabilities, the form and the area of the front will differ significantly from the situation with homogeneous permeability. The redistribution of the flow rate in the computational domain leads to evolution of the stationary front and accordingly to a change in the temperature field. The calculations showed that use of nonuniform permeability enables us to alter the filtration conditions so that emitting surface II is washed better by the hot gas. The temperature distribution on this surface becomes more uniform, which improves the emitting properties of the technical device. This model makes it possible to control the temperature-field distribution and the flow profile by using systems with nonuniform properties.

CONCLUSIONS

1. The developed two-dimensional numerical model enables us to analyze the stability of combustion with a stationary front and the thermal regimes in devices of variable cross section filled with an inhomogeneous porous charge with gas filtration in direct-current flow and with a turn of the gas flow.

2. In the case where this system is stable, the area of the surface on which the combustion occurs agrees to a good degree of accuracy with the analytical evaluation obtained in a one-dimensional theory.

NOTATION

c, specific heat; C, dimensionless concentration of the fuel; D, diameter of the charge grains; U, activation energy; k, permeability of the porous mediun; K, preexponential factor; H, heat of combustion of the fuel mixture; P, pressure; p_0, atmospheric pressure; R_g, universal gas constant; S, area; t, time; T, temperature; α, coefficient of convective heat transfer; ρ, density; u, filtration rate; ε, emissivity factor; ε_p, bulk porosity; λ, thermal conductivity; μ, dynamic viscosity; σ, Stefan–Boltzmann constant. Subscripts: ad, adiabatic conditions; g, gaseous phase; m, charge material; s, solid phase; in, inlet; num, numerical; out, outlet; turn, turn; I ... VII, numbers of boundaries; 0, ambient medium; 1, quantity determined analytically.

REFERENCES

1. S. Zhdanok, L. A. Kennedy, and G. Koester, Combust. Flame, **100**, 221-231 (1995).
2. D. A. Frank-Kamenetskii, Diffusion and Heat Transfer in Chemical Kinetics [in Russian], Moscow (1980).
3. V. S. Babkin, Pure Appl. Chem., **65**, 335-344 (1993).
4. S. I. Fut'ko, S. I. Shabunya, and S. A. Zhdanok, Inzh.-Fiz. Zh., **71**, No. 1, 41-45 (1998).
5. M. É Aérov, O. M. Todes, and D. A. Narinskii, Apparatuses with a Granular Bed [in Russian], Leningrad (1979).
6. S. A. Zhdanok, V. V. Martynenko, and S. I. Shabunya, Inzh.-Fiz. Zh, **64**, No. 5, 569-576 (1993).
7. Y. Yoshizava, H. Sasaki, and R. Echigo, Proc. National Heat Transfer Conference (ASME Paper 87-HT-57) (1987), pp. 1-5.
8. K. Hanamura, R. Echigo, and S. Zhdanok, Int. J. Heat Mass Transfer, **36**, No. 13, 3201-3209 (1993).
9. O. S. Rabinovich, A. V. Fefelov, and N. V. Pavlyukevich, 26th Intern. Symp. on Combustion, The Combustion Institute, Pittsburgh, PA, Vol. 2 (1997), pp. 3383-3389.